Singlet-triplet anticrossings between the doubly excited 3 1K state and the g (3d) 3Sigma + g state of H2

Robert S. Freund, Terry A. Miller, R. Jost, M. Lombardi

Singlet–triplet anticrossings between the doubly excited $3\,^1K$ state and the $g(3d)^3\Sigma_g^+$ state of H_2

Robert S. Freund[a] and Terry A. Miller[a]

Bell Laboratories, Murray Hill, New Jersey 07974

R. Jost[b] and M. Lombardi[b]

Laboratoire de Spectrometrie Physique, [c] *Universite Scientifique et Medicale de Grenoble, B.P. 53-38041, Grenoble, France*

(Received 12 October 1977)

The $3\,^1K$, $v=1$ level of H_2 has recently been interpreted as an adiabatic mixture of vibronic levels of the $EF\,^1\Sigma_s^+$ and the $GK\,^1\Sigma_g^+$ double minimum states, with currently undetermined nonadiabatic corrections. Anticrossing spectra, which are sensitive to these state mixings, have been observed for the $3\,^1K$, $v=1$, N level and the $(3d)^3\Sigma_g^+$, $v=1$, N level of ortho-H_2 for the rotational levels $N=1$ and 3. Linewidths, which are determined by either the singlet–triplet Fermi-contact hyperfine interaction or the spin–orbit interaction, as well as magnetic g values, help provide a detailed description of the $3\,^1K$ state. Measured singlet–triplet zero field separations are combined with previously published values to provide the best available value for the energy $T_0(a\,^3\Sigma)$ of the lowest triplet level ($a\,^3\Sigma$, $v=0$, $N=0$) with respect to the ground state, 95076.36 ± 0.20 cm^{-1}.

I. INTRODUCTION

Although Richardson, in his classic 1934 monograph,[1] was able to explain much of the H_2 spectrum, a number of bands defied interpretation. They were certainly due to singlet states as their lower state combination differences all fit the $B(2p)\,^1\Sigma_u^+$ state. Since bands from all possible one-electron-excited configurations had been identified, this left no alternative but to assign the remaining bands to two-electron excited configurations. Thus Richardson[1] and Dieke[2–4] list a number of doubly excited states, and identify them by symbols such as $3\,^1K$, ^1L, ^1N, etc.

The first major advance in understanding doubly excited states came in 1960 when Davidson[5] showed by an *ab initio* calculation that the lowest excited $^1\Sigma_g^+$ state possesses a double minimum, with the inner minimum having a configuration primarily $(1s\sigma, 2s\sigma)$ and the outer minimum being largely $(2p\sigma)^2$. Thus the previously identified $E\,^1\Sigma_g^+$ and $F\,^1\Sigma_g^+$ states were shown to result from vibrational levels in different parts of the same electronic potential. A subsequent calculation by Kolos and Wolniewicz[6] obtained near quantitative agreement with the experimental levels[7] of the $E, F\,^1\Sigma_g^+$ double minimum state.

The situation with the higher lying doubly excited states ($3\,^1K$, ^1L, ^1N, etc.) remained confused, although it was suggested that their interpretation involved higher double minimum states.[5,8] The most recent advances have been made by Glover and Weinhold[9] and by Wolniewicz and Dressler,[10] who computed potential curves for the second excited $^1\Sigma_g^+$ state which they call the GK state since the lower vibrational levels of the inner minimum are the $G(3d)\,^1\Sigma_g^+$ state and the outer minimum is related to the $3\,^1K$ state. Wolniewicz and Dressler[10] have, in addition, calculated vibrational energy levels for the EF and GK states all the way to the dissociation limit, and have considered nonadiabatic perturbations between these states.[11] In this way they can interpret the observed "doubly excited" singlet states, and so bring order to a situation which was chaotic for almost 50 years. In their preliminary nonadaibatic analysis Wolniewicz and Dressler[11] find that the $v=1$ level of $3\,^1K$ corresponds to the wavefunction $-0.79\,EF22 + 0.58\,GK3$ + smaller contributions (where $EF22$ is the 22nd vibrational level of the EF state, etc.), that is, a strong mixture of adiabatic states. (For convenience, we shall continue to refer to it as the state identified by experiment, $3K_1$.) It is important to test this analysis against all possible experimental data, especially for the strongly perturbed levels.

In this paper we present the results of anticrossing measurements between the $g(3d)\,^3\Sigma_g^+$, $v=1$ level and the $3\,^1K$, $v=1$ level ($3K_1$). Anticrossing spectroscopy[12,13] permits measurement of the zero-magnetic field separation between two levels, the strength of the perturbation between them, and their g values. These last two properties should serve to test the theoretical interpretation of the $3K_1$ level. The first property, the zero field separation $h\nu_0$, helps to more precisely define the separation between the singlet and triplet levels of H_2.

II. EXPERIMENTAL

This set of anticrossings was first observed independently by the Grenoble group and at M.I.T. by the Bell Labs group. The apparatuses have been described before.[14,15] Briefly, the Grenoble group excites H_2 in a sealed cell by radiofrequency power, whereas the Bell Labs group flows H_2 and excites it with an electron beam. Both groups use Bitter coils to attain the required high magnetic field.

---

[a] Part of this work was performed while the authors were guest scientists at the Francis Bitter National Magnet Laboratory, which is supported at M.I.T. by the National Science Foundation.

[b] Work performed in part at the Service National des Champs Intenses of Grenoble (Centre National de la Recherche Scientifique), France.

[c] Laboratoire associé au Centre National de la Recherche Scientifique.

 0021-9606/78/6804-1683$01.00

Final measurements were made at M.I.T. using the Bitter magnet without stabilization. The magnetic field was measured with a Hall probe which was calibrated with respect to an NMR several times while making measurements. The estimated accuracy of the magnetic field measurements is ±50 G below 90 kG and ±100 G between 90 and 120 kG, where the estimates include several sources of error, i.e., Hall probe calibration, line center determination for a broad line in a limited number of observations, etc.

Prepurified grade H_2 flowed directly from a cylinder and was maintained at a pressure of 20 mTorr in the interaction region. The electron beam had a 60 mA current and an energy ranging between 40 and 80 eV. Monochromator resolution was 4 Å for most measurements, although resolution down to 1 Å was used to make spectral assignments. An EMI 6256 photomultiplier was used for all but one line, which was in the red and so required an EMI 9558. Count rates were generally about 10^5 sec^{-1}.

III. RESULTS

A. Measurements

Anticrossings were observed on the optical lines listed in Table I. Observations of signals with the same width and center field, but at wavelengths corresponding to different rotational or vibrational transitions from the same upper level, confirm the singlet quantum number assignments. Observation of an inverted anticrossing on a triplet state emission line confirms the assignment of that state. The good fit to theory found below provides a further check on the assignments.

The appropriate energy level diagrams are given in Figs. 1 and 2. The $h\nu_0$ and the g values needed to construct these figures have been taken from the results of this experiment. The $^3\Sigma$ fine structure is too small to represent on this scale. Hyperfine structure is omitted except in the two inserts which illustrate its effect. As the dominant hyperfine interaction is Fermi contact, we do not consider the nuclear spin–electron spin dipolar or the nuclear spin–electron orbital interactions. Thus the hyperfine energy is approximated by $a_F M_I M_S$. This

TABLE I. Optical transitions on which anticrossings have been observed. Most measurements were made on the lines marked by asterisks.

Transition	Band	Line	λ_{air}(Å)
$3\,^1K \rightarrow 2p\,^1\Sigma_u^+$	1–0	RO	4222.5
	1–1	$P2$	4493.7
	1–3	$P2$	5067.5*
$3\,^1K \rightarrow 2p\,^1\Sigma_u^+$	1–0	$R2$	4223.9
	1–1	$R2$	4472.0
	1–3	$R2$	5039.8
	1–3	$P4$	5099.7*
$3d\,^3\Sigma_g^+ \rightarrow 2p\,^3\Pi_u$	1–1	$Q1$	6021.3

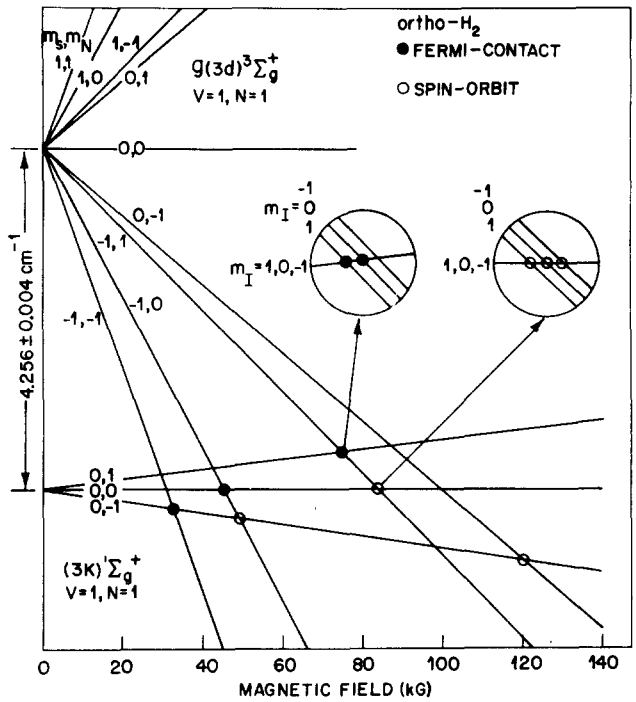

FIG. 1. Energy level diagram of the $N=1 \leftrightarrow N=1$ anticrossings.

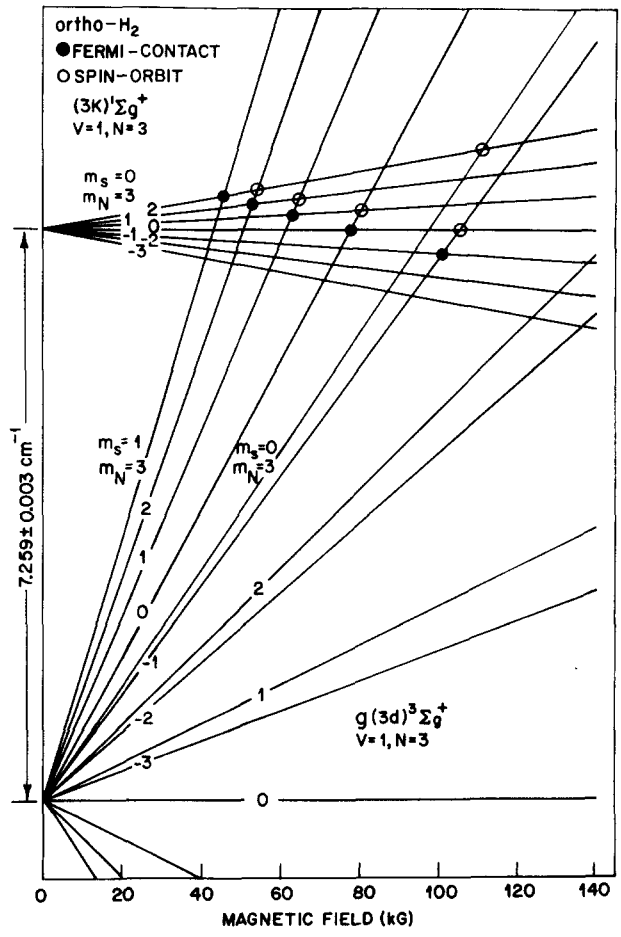

FIG. 2. Energy level diagram of the $N=3 \leftrightarrow N=3$ anticrossings.

expression vanishes in all singlet states and gives an evenly spaced triplet in triplet states.

Two dominant singlet–triplet interactions give rise to the observed anticrossings, spin–orbit and Fermi contact. For an anticrossing to occur, the value of $M_F(=M_S+M_N+M_I)$ must be the same in both levels. Fermi-contact perturbations give the selection rules $\Delta M_I=-\Delta M_S=\pm 1$ and $\Delta M_N=0$, whereas spin–orbit perturbations give $\Delta M_N=-\Delta M_S=0,\ \pm 1$ and $\Delta M_I=0$.

Each anticrossing was measured by signal averaging 4 scans of a 4–8 kG region, the entire run lasting about 10 min. The magnetic field was calibrated by the Hall probe immediately after each measurement. The measured anticrossing position and assignments are given in Table II. The one standard deviation uncertainties are dominated by scatter in the measurements, although the contributions from the Hall probe uncertainties are not negligible. Limited running time with the Bitter magnet precluded more extensive measurements.

As the inserts to Fig. 1 show, each observed anticrossing is actually a blend of two or three unresolved hyperfine components. Rather than include hyperfine structure explicitly in our fitting routines, we make the necessary small adjustments to the line position and then use a simplified fitting model. The three equally spaced spin–orbit allowed anticrossings require no adjustment. For the Fermi-contact perturbation, however, only two of the three potential anticrossings occur. The observed anticrossing field must be adjusted upward by $a_F/2\mu_0 g_{eff}$ G, where the effective g value for the anticrossing is given by

$$g_{eff}=\left|g_S M_S^t+g_N^t M_N^t-g_N^s M_N^s\right|. \tag{1}$$

a_F is determined primarily by the $1s\sigma_g$ electron and so has a value of 450 MHz in $v=1$ of the triplet state.[16] The adjusted line positions are given in Table II.

B. Energy level fit

The magnetic field H at which anticrossing occurs is that field for which the singlet and triplet energies become equal. That is:

$$E_T-E_S=0=h\nu_0+\mu_0 H[g_S M_S^t+g_N^t M_N^t-g_N^s M_N^s]$$
$$-A' M_N^t+SS[3(M_N^t)^2-6]+\mathrm{CH}^2(M_N^t)^2+\mathrm{DH}^2(M_N^s)^2+\mathrm{EH}^2\ . \tag{2}$$

$h\nu_0$ is the zero field separation between triplet and singlet $(E_T^0-E_S^0)$. g_S is the electron spin g factor; its value is fixed at the free electron value 2.00232 in this work. M_S and M_N are the spin and rotational magnetic quantum numbers, respectively, where the superscript indicates singlet or triplet. g_N in the rotational g factor A' and SS describe the spin–orbit and spin–spin fine structure, respectively. The last three terms describe the quadratic Zeeman interaction in the most general way possible.

For the $N=1\rightarrow N=1$ anticrossings, there are only six observed anticrossings but a possible eight variable parameters. Some of these parameters must be omitted from the fit. Three parameters, $h\nu_0$, g_N^s, and g_N^t, largely determine the spectrum. A least squares fit in which the three dominant parameters are varied and the five less significant parameters are fixed at zero, however, could not fit the six measurements to within the experimental uncertainty; the residual (observed minus calculated) field positions were roughly 4 times larger than the uncertainties. Five additional fits were therefore tried; in each of them, one of the remaining 5 parameters was allowed to vary. Four of them gave residuals about a factor of 2 smaller than those from the three parameter fit, as one might expect from the additional degree of freedom in the fit. When C was varied, however, the residuals fell to values comparable to or smaller than the experimental uncertainties. The resulting parameter values are given in Table III and the residuals in Table II.

TABLE II. Quantum number assignments, measurements, and corrected measurements. *FC* and *SO* indicate anticrossings allowed by Fermi-contact and spin–orbit perturbations, respectively.

	$g(3d)\,^3\Sigma_g^+$ $v=1$		$3\,^1K$ $v=1$									
$N=N'$	M_S	M_N	M_S	M_N	Perturbation	Observed position (G)	g_{eff}	Position corr. for hyperfine	Residual (obs–calc) (G)	Observed width (G)	Width of comp. (G)	Width of comp. MHz ±10%
1	−1	−1	0	−1	*FC*	32 870 ± 60	2.764	32 930	8	368 ± 34	309	1195
1	−1	0	0	0	*FC*	45 390 ± 50	2.002	45 470	−63	544 ± 3	468	1310
1	−1	0	0	−1	*SO*	49 470 ± 50	1.844	49 470	49	1076 ± 80	954	2455
1	−1	1	0	1	*FC*	72 910 ± 80	1.240	73 040	55	757 ± 49	610	1056
1	−1	1	0	0	*SO*	83 370 ± 150	1.082	83 370	−49	1748 ± 89	1529	2301
1	0	−1	0	−1	*SO*	117 200 ± 210	0.762	117 200	0	2152 ± 167	1808	1931
3	0	3	1	3	*FC*	45 730 ± 40	3.400	45 680	80	367 ± 4	328	1538
3	0	2	1	2	*FC*	53 060 ± 40	2.934	53 000	18	425 ± 8	380	1543
3	0	3	1	2	*SO*	54 180 ± 40	2.870	54 180	28	643 ± 116	559	2222
3	0	1	1	1	*FC*	63 120 ± 50	2.468	63 050	−36	480 ± 33	423	1451
3	0	2	1	1	*SO*	64 680 ± 40	2.404	64 680	22	811 ± 126	715	2391
3	0	0	1	0	*FC*	77 810 ± 50	2.002	77 730	−74	583 ± 86	512	1434
3	0	1	1	0	*SO*	80 290 ± 50	1.938	80 290	−54	1107 ± 62	1000	2715
3	0	−1	1	−1	*FC*	101 250 ± 120	1.536	101 150	12	692 ± 62	591	1282
3	0	0	1	−1	*SO*	105 580 ± 120	1.472	105 580	4	1531 ± 82	1402	2923
3	0	3	0	3	*SO*	111 500 ± 120	1.398	111 500	−102	1995 ± 182	1870	3534

TABLE III. Parameter values resulting from least squares fits to the data. The uncertainties represent one standard deviation.

	$N=1$	$N=3$
$h\nu_0$(MHz)	127600 ± 110	−217630 ± 100
(cm^{-1})	4.256 ± 0.004	−7.259 ± 0.003
g_N^s	0.158 ± 0.002	0.064 ± 0.001
g_N^t	0.920 ± 0.002	0.530 ± 0.001
g_S	2.00232(fixed)	2.00232(fixed)
C(mHz/G^2)	−180 ± 30	0(fixed)

For the $N=3 \rightarrow N=3$ anticrossings there are 10 observed anticrossings and only eight parameters, so in principle all of the parameters can be determined. We found, however, that the spectrum can be fit to within the experimental uncertainties by varying only the three major parameters. The results are given in Tables II and III. Variation of additional parameters gave residuals smaller than the experimental uncertainties, implying that noise was being fit.

C. Linewidths

The observed linewidths (Table II) are each the average of from two to six independent measurements. Temporal instability of the magnetic field is only about 1 part in 10^3, so its contribution to the reported linewidths is ignored. The stated uncertainties are one standard deviation of the measurements. The observed widths fall roughly into two groups, smaller widths for the Fermi-contact anticrossings and larger widths for the spin–orbit anticrossings. As each observed line is a blend of closely spaced components (two for Fermi contact and three for spin–orbit), the widths of individual components have been calculated by adding Lorentzian lines with fixed separations and variable widths so that the observed widths are reproduced. The resulting component widths are given in Table II. Finally, the component widths in MHz are given by the width in gauss, divided by $\mu_0 g_{eff}$. The uncertainties, we feel, are better estimated as 10%, rather than as the standard deviations of the measurements, some of which appear to be fortuitously small.

IV. DISCUSSION

A. Singlet–triplet interaction strengths

The singlet–triplet interaction matrix elements V_{ST} which give rise to the anticrossings also essentially determine the widths of the anticrossings. In the limit of a strong interaction, the radiative lifetime contribution to the width is negligible, and the linewidth is given by[17]

$$\Delta\nu = 4\,|V_{ST}| \ . \tag{3}$$

As in Ref. 17, the two major interactions are Fermi-contact hyperfine and spin–orbit perturbations.

The respective linewidths are given by

$$\Delta\nu_{FC} = 4\,|V_{ST}| = 4\,\tilde{a}_F \langle I_T, 1, M_I, \pm 1 \,|\, I_T, M_I \pm 1\rangle\, \delta_{M_N, M_{N'}} [I_T(I_T+1)]^{1/2} \tag{4}$$

and

$$\Delta\nu_{SO} = 4\,|V_{ST}| = 4\,\langle \tilde{AL}\rangle_{ST} \langle N, 1, M_N, q \,|\, N, M_N + q\rangle \delta_{M_I, M_I'} \ , \tag{5}$$

where the Fermi-contact and spin–orbit parameters a_F and $\langle \tilde{AL}\rangle_{ST}$, respectively, are defined in Ref. 17.

$\tilde{a}_F$ can be evaluated from Eq. (4) and the linewidths in Table II. We first evaluate $\tilde{a}_F$ for each anticrossing and then average the results to get $\tilde{a}_F = 338 \pm 34$ MHz, where the quoted error is based upon the individual 10% uncertainties. As the spin–orbit parameter $\langle \tilde{AL}\rangle_{ST}$ is dependent on N, we report different values for $N=1$ and $N=3$. The $N=1$ value is 788 ± 97 MHz and the $N=3$ value is 1010 ± 113 MHz.

The most striking thing about these parameter values is their large size. The Fermi-contact interaction lends itself to the most direct interpretation. Because of the nature of the Fermi-contact operator, one would theoretically expect it to be about the same for all singly excited triplet states of H_2 as it is primarily determined by the $1s\sigma_g$ electron. Experimental confirmation of this hypothesis has been obtained[16,17] for the $c(2p)\,^3\Pi_u$, $d(3p)\,^3\Pi_u$, and $f(4p)\,^3\Sigma_u^+$ states where it is ~ 450 MHz. Likewise, one can argue theoretically that $\tilde{a}_F$ between singly excited singlet and triplet states should be the same as the diagonal $\tilde{a}_F$ in the triplet states. Recently, this hypothesis has been confirmed by measurement[18] of $\tilde{a}_F$ between the $v=1$ levels of the $G(3d)\,^1\Sigma_g^+$ and $g(3d)\,^3\Sigma_g^+$ states of D_2, which when scaled by the H/D nuclear g factors gives a value of $\tilde{a}_F = 477 \pm 74$ MHz, in a situation where the vibrational overlap is presumably very near unity.

Our present experimental result for $\tilde{a}_F$ is ~ 75% of the "standard" value of 450 MHz. The result is quite inexplicable in terms of the old interpretation of the $3\,^1K$ state as having solely a doubly excited configuration, both because of the absence of a $1s\sigma_g$ orbital to give a large electronic integral and the likely very bad vibrational overlap between such a state and the $g(3d)\,^3\Sigma$ state. The recent interpretations of the $3\,^1K$ as having substantial $3d$ character are much more consistent with the present result. However, we note that the adiabatic linear combination, $-0.79\,EF22 + 0.58\,GK3$, still seems unlikely to give as large a value for $\tilde{a}_F$ as is experimentally observed. Indeed, the present result should serve as a sensitive test of the nonadiabatic mixing of the levels of the EF and GK states when a complete calculation is available.

Interpretation of $\langle \tilde{AL}\rangle_{ST}$ is less straightforward, as it depends critically on the degree of L uncoupling in both the singlet and triplet states. It is nonetheless surprising (but consistent with the present hyperfine results) that the present values in the $N=1$ and 3 levels are as large as the 813 MHz value between the

TABLE IV. Determinations of $T_0(a\,^3\Sigma)$ for H_2 from this and previous work. (cm^{-1}).

Singlet state	Triplet state	$E^t - E^s$	E^s	$T_0 - E^t$	$T_0(a\,^3\Sigma)$	Reference
$R(4d)\,^1\Pi_g$ $v=1$, $N=4$	$r(4d)\,^3\Pi_g$ $v=1$, $N=4$	1.42	120 031.61	−24 956.58	95 076.45	13
$J(3d)\,^1\Delta_g$ $v=1$, $N=3$	$j(3d)\,^3\Delta_g$ $v=1$, $N=3$	1.14	114 923.56	−19 848.30	95 076.40	12, 13
$W(?)\,^1\Sigma_g^+$ $v=1$, $N=4$	$i(3d)\,^3\Pi_g$ $v=1$, $N=6$	1.45	115 450.32	−20 375.33	95 076.44	13, 20
$G(3d)\,^1\Sigma_g^+$ $v=0$, $N=2$	$g(3d)\,^3\Sigma_g^+$ $v=0$, $N=2$	−1.24	111 827.84	−16 750.23	95 076.37	12
$G(3d)\,^1\Sigma_g^+$ $v=0$, $N=3$	$g(3d)\,^3\Sigma_g^+$ $v=0$, $N=3$	3.5	111 893.13	−16 820.32	95 076.3	12
$B'(3p)\,^1\Sigma_u^+$ $v=3$, $N=0$	$f(4p)\,^3\Sigma_u^+$ $v=0$, $N=0$	−4.28	115 606.45	−20 525.92	95 076.25	15
$B'(3p)\,^1\Sigma_u^+$ $v=3$, $N=1$	$f(4p)\,^3\Sigma_u^+$ $v=0$, $N=1$	4.94	115 647.12	−20 575.64	95 076.42	15
$3\,^1K$ $v=1$, $N=1$	$g(3d)\,^3\Sigma_g^+$ $v=1$, $N=1$	4.26	113 879.40	−18 807.41	95 076.25	This work
$3\,^1K$ $v=1$, $N=3$	$g(3d)\,^3\Sigma_g^+$ $v=1$, $N=3$	−7.26	113 987.60	−18 904.02	95 076.32	This work
			Average $T_0(a\,^3\Sigma_g^+) = 95\,076.36 \pm 0.20$			

$G(3d)\,^1\Sigma_g^+$ and the $g(3d)\,^3\Sigma_g^+$ states[18] where the vibrational overlap should be near unity.

B. g values

As both the singlet and triplet states in this experiment are Σ states, they would have zero g values if case b were appropriate. Their large nonzero values imply the importance of L uncoupling. Were L uncoupling complete (Hund's case d), the $3d\,^3\Sigma$ g values would be 1.5 for $N=1$ and 2/3 for $N=3$. A simple calculation of the $3d\,^3\Sigma$ g values has been made from the intermediate case wavefunction, obtained by considering only the $3d\,^3\Sigma$, $3d\,^3\Pi$, and $3d\,^3\Delta$ states with $v=1$. The results are 0.917 and 0.568 for $N=1$ and 3, respectively, in close agreement with experiment, indicating that the dominant interactions involve these three states.

The $3K$ state g values have the same limits as for the $3d\,^3\Sigma$ state, but in actuality are more difficult to interpret because of the nonadiabatic nature of the levels and their interactions with $3s$ and $3d$ singlet states. Using preliminary values[11] for the L-uncoupling integrals to only the $3d\,^1\Pi$ states we obtain calculated g values of 0.25 and 0.16 for $N=1$ and 3, respectively. We note that the qualitative agreement between theory and experiment is not bad, but we stress the preliminary nature of this result and leave detailed interpretation of these $3K$ g values to future work which can utilize more refined calculations of the nonadiabatic levels.

C. Zero-field separations

Comparison of the zero-field separation $h\nu_0$ to an optical value cannot be carried out directly, as no singlet–triplet optical transition has every been reported in H_2. A useful comparison, therefore, is to combine optical measurements with the anticrossing result, and thereby determine the energy $T_0(a\,^3\Sigma)$ of the lowest triplet level ($a\,^3\Sigma$, $v=0$, $N=0$) with respect to the ground state. Such a calculation has been presented previously for D_2.[19] In Table IV we present the results for H_2. Results for all previously reported singlet–triplet anticrossings in H_2 are included,[12,13,15,20] since they have not been collected previously in this form. Differences in T_0 result from errors of the order of 0.1 cm^{-1} in the optically determined energy levels. There may be a slightly larger systematic error in T_0 due to the uncertainty of the vacuum uv measurements which position all excited singlets with respect to the ground state. We estimate the combined error as ± 0.2 cm^{-1}.

[1] O. W. Richardson, *Molecular Hydrogen and Its Spectrum* (Yale U. P., New Haven CT, 1934).
[2] G. H. Dieke, Phys. Rev. **50**, 797 (1936).
[3] G. H. Dieke, Phys. Rev. **76**, 50 (1949).
[4] G. H. Dieke, J. Mol. Spectrosc. **2**, 494 (1958).
[5] E. R. Davidson, J. Chem. Phys. **33**, 1577 (1960); **35**, 1189 (1961).
[6] W. Kolos and L. Wolniewicz, J. Chem. Phys. **50**, 3228 (1969).
[7] G. H. Dieke and S. P. Cunningham, J. Mol. Spectrosc. **18**, 288 (1965).
[8] G. B. Field, W. B. Somerville, and K. Dressler, Ann. Rev. Astron. Astrophys. **4**, 207 (1966).
[9] R. M. Glover and F. Weinhold, J. Chem. Phys. **66**, 303 (1977).
[10] L. Wolniewicz and K. Dressler, J. Mol. Spectrosc. **67**, 416 (1977).
[11] K. Dressler (private communication).
[12] R. Jost and M. Lombardi, Phys. Rev. Lett. **33**, 53 (1974).
[13] T. A. Miller and R. S. Freund, J. Chem. Phys. **61**, 2160 (1974).
[14] J. Derouard, R. Jost, M. Lombardi, T. A. Miller, and R.

S. Freund, Phys. Rev. A **14**, 1025 (1976).
[15]T. A. Miller and R. S. Freund, J. Mol. Spectrosc. **63**, 193 (1976).
[16]R. S. Freund and T. A. Miller, J. Chem. Phys. **59**, 5770 (1973).
[17]T. A. Miller and R. S. Freund, J. Mol. Spectrosc. **63**, 193 (1976).
[18]T. A. Miller, B. R. Zegarski, and R. S. Freund, J. Mol. Spectros. (to be published).
[19]R. Jost, M. Lombardi, J. Derouard, R. S. Freund, T. A. Miller, and B. R. Zegarski, Chem. Phys. Lett. **37**, 507 (1976).
[20]T. A. Miller and R. S. Freund, J. Chem. Phys. **63**, 256 (1975).